ADVANCES IN THE THEORY OF VOLUME REFLECTION AND THE ACCOMPANYING RADIATION

M.V. Bondarenco

KIPT, Kharkov, Ukraine

Contents

I. Model solution for volume reflection in a uniformly bent crystal

- Analytic expressions for mean deflection angle and the final beam shape
- Comparison with experiments

[M.V. Bondarenco. PRA, accepted for publication]

II. Coherent bremsstrahlung in an arbitrarily bent crystal

- Analytic expression for radiation spectrum
- Comparison with experiments

[M.V. Bondarenco. PRA, **81** (2010) 052903]

[M.V. Bondarenco. J. Phys.: Conf. Ser. **236** (2010) 012026]

I. Volume reflection

An exactly solvable model for volume reflection in silicon crystals is found, based on parabolic approximation for the inter-planar potential, and with the neglect of multiple scattering.

Volume reflection was discovered in numerical simulations 2 decades ago [Taratin & Vorobiev, 1987] as a phenomenon of over-barrier fast charged particle deflection to the side opposite to that of the crystal bending. It was further suggested for use in beam splitters and collimators at high-energy accelerators.

In general, the particle motion in the intra-crystal field is rather complicated, which fostered further numerical simulation research. But in the commonly used silicon material ($Z=14<<137$) the inter-planar averaged potential is close to parabolic (whereas multiple scattering is negligible in sufficiently thin crystals). Employing this approximation, it becomes possible to solve the equations of motion not only in a single inter-planar cell, but through the entire bent crystal, and analytically perform the corresponding averaging procedures.

The limiting values for the deflection angle were derived to equal $\pi/2$ for positively charged particles, and 1 for negatively charged particles, in units of the Lindhard critical angle. The model also nicely describes departures from the limiting values, as measured by 2009 CERN experiment with protons.

Thin bent crystals. Geometry of passage

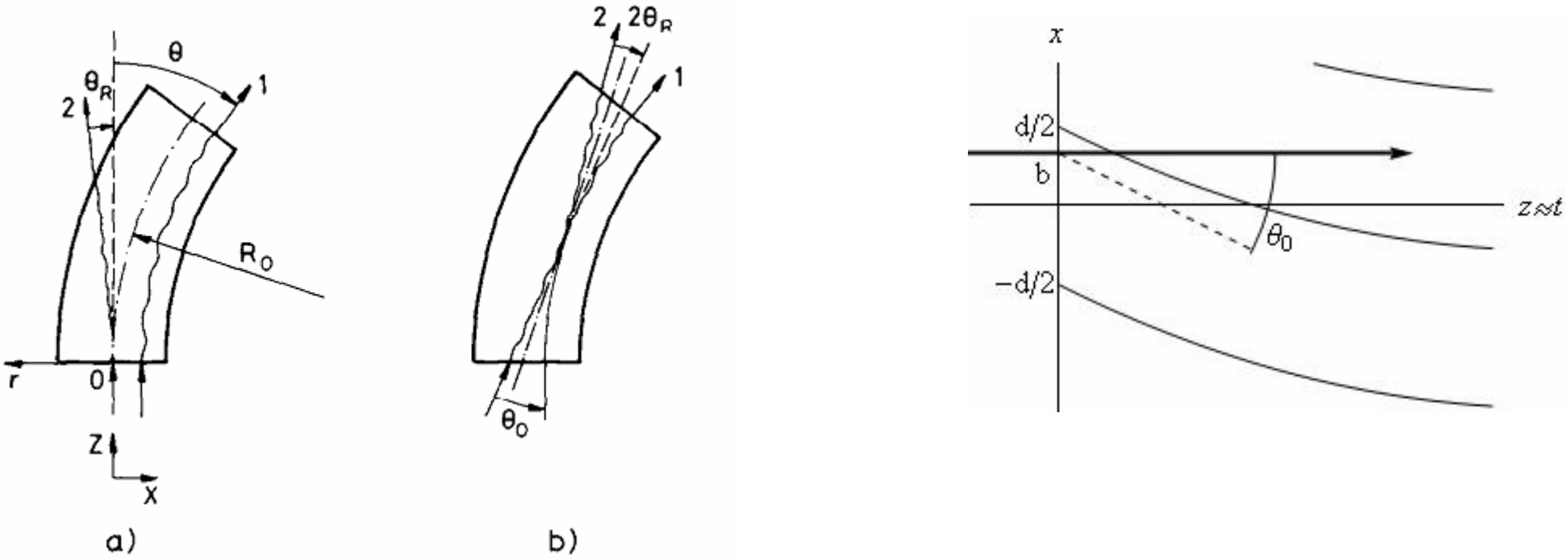

(Figure from [Taratin & Vorobiev, 1987])

Final beam shapes in cases a) and b) are not homomorphic.

Experimentally, more relevant is case b).

Boundary (initial) conditions: $\left.\begin{aligned} x(0) &= b \\ \dot{x}(0) &= 0 \end{aligned}\right\}$ AFTER the entrance to the crystal.

I.e., no refraction on the crystal boundary, only a (b-dependent) potential jump.

Equations of motion and the solution

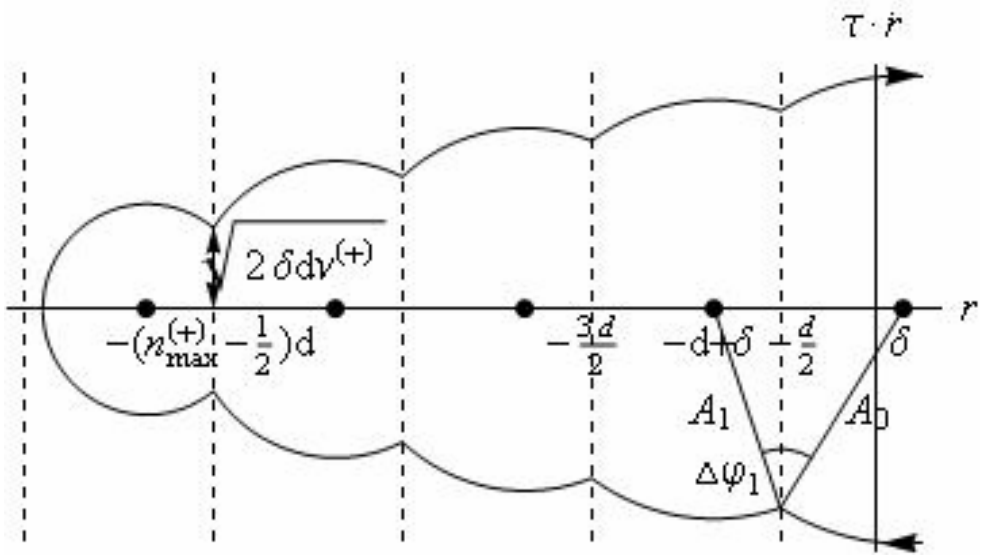

$$r_n(t) = \pm\delta - nd - A_n \begin{Bmatrix}\sin\\ \sinh\end{Bmatrix}\left(\frac{t}{\tau} + \varphi_0 + \sum_{m=1}^{n}\Delta\varphi_m\right) \quad \text{(valid at } -\frac{d}{2} - nd \le r \le \frac{d}{2} - nd,\ \ t_n \le t \le t_{n+1}\text{)}$$

$$A_n = \sqrt{A_{n-1}^2 - 2\delta d} = \sqrt{A_0^2 - 2n\delta d}$$
$$= \sqrt{\tau^2\theta_0^2 \pm (b \pm \delta)^2 - 2\delta d}$$

$$\Delta\varphi_n = -\begin{Bmatrix}\arcsin\\ \operatorname{arsinh}\end{Bmatrix}\frac{\frac{d}{2} \pm \delta}{A_{n-1}} - \begin{Bmatrix}\arcsin\\ \operatorname{arsinh}\end{Bmatrix}\frac{\frac{d}{2} \mp \delta}{A_n}$$

Not a recursive procedure. Gives an explicit expression for the trajectory in an arbitrary interval. (Because of the existence of an (transverse energy) integral of motion.)

Closed-form expression for the final deflection angle

$$\frac{t_{\text{refl}}}{\tau} = \frac{\pi}{2} + \sum_{n=1}^{n_{\max}^{(+)}} \left(\arcsin \frac{\frac{d}{2}+\delta}{A_{n-1}} + \arcsin \frac{\frac{d}{2}-\delta}{A_n} \right) - \arcsin \frac{b+\delta}{A_0}, \qquad \theta = 2 \lim_{\theta_0/\theta_c \to \infty} \left(-\theta_0 + \delta \frac{t_{\text{refl}}(\theta_0)}{\tau^2} \right)$$

Comparison with the general integral representation for the deflection angle in a centrally-symmetric field

$$\theta \approx \frac{1}{R} \int_{r_{\min}}^{\infty} \frac{dr}{\sqrt{\frac{\theta_0^2}{4} + \frac{V_{\text{eff}}(b) - V_{\text{eff}}(r)}{2E}}}$$

(used by [Taratin & Vorobiev, 1987], [Maisheev, 2007])

Substituting here the parabolic approximation for V, and partitioning the integration interval to individual inter-planar intervals, one retrieves the same sum of arcsines:

$$\int_{-d/2-nd}^{d/2-nd} \frac{dr}{\sqrt{\tau^2\theta_0^2 + b^2 + 2\delta(b+r) - (r+nd)^2}} = \arcsin \frac{\frac{d}{2}-\delta}{\sqrt{\tau^2\theta_0^2 + (b+\delta)^2 - 2n\delta d}} + \arcsin \frac{\frac{d}{2}+\delta}{\sqrt{\ldots}}$$

But for future studies of inelastic processes (radiation, incoherent multiple scattering, volume capture, etc.), it is necessary to have an expression not only for the final elastic deflection angle, but for the whole trajectory. The geometric interpretation for arcsine arguments is also useful.

Further analytic procedure

1. At $R \gg R_c$, when the number of terms in the sum gets large, replace the sums by integrals.
2. Do the encountered integrals in closed form.
3. Invert the dependence $\theta(b)$, derive the differential cross-section $\frac{d\lambda}{d\theta} = b'(\theta)$.
4. Average the differential cross-section over (small interval of) θ_0.

(So many tasks to manage – rather, the analytic (model-based) approach only begins at this stage!)

Results for positively charged particles

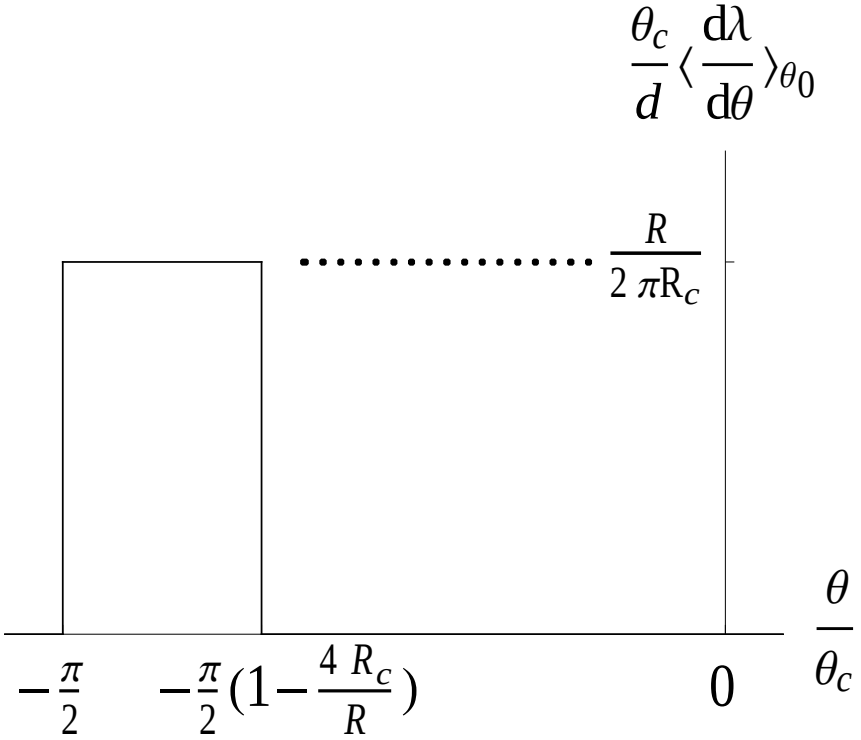

Comparison with CERN experiment, 2009

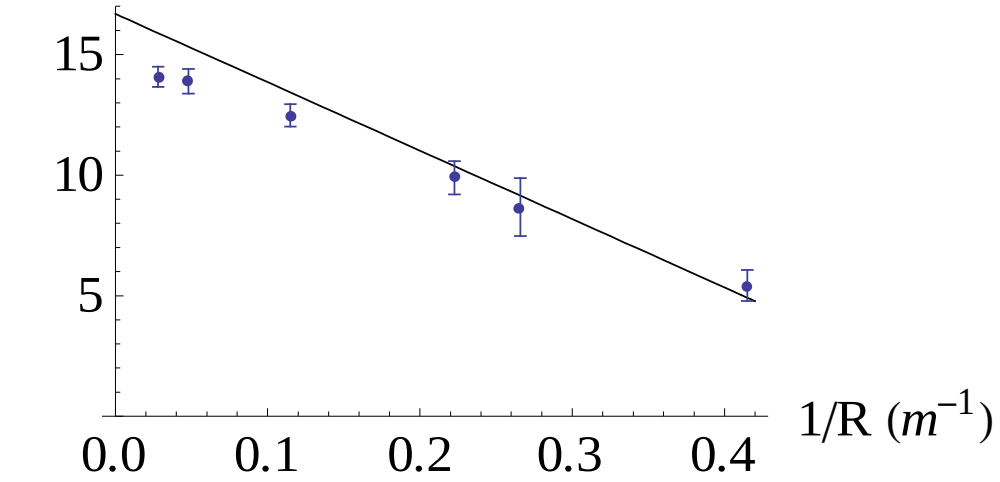

$\left|\langle\theta\rangle\right| = \frac{\pi}{2}\theta_c\left(1-\frac{2R_c}{R}\right)$ – the mean value is least sensitive to incoherent multiple scatterings in the target

$\left.\begin{aligned}\theta_c &= \sqrt{2V_0/E}\\ R_c &= \frac{Ed}{4V_0}\end{aligned}\right\}$ are better expressed in terms of V_0

Results for negatively charged particles

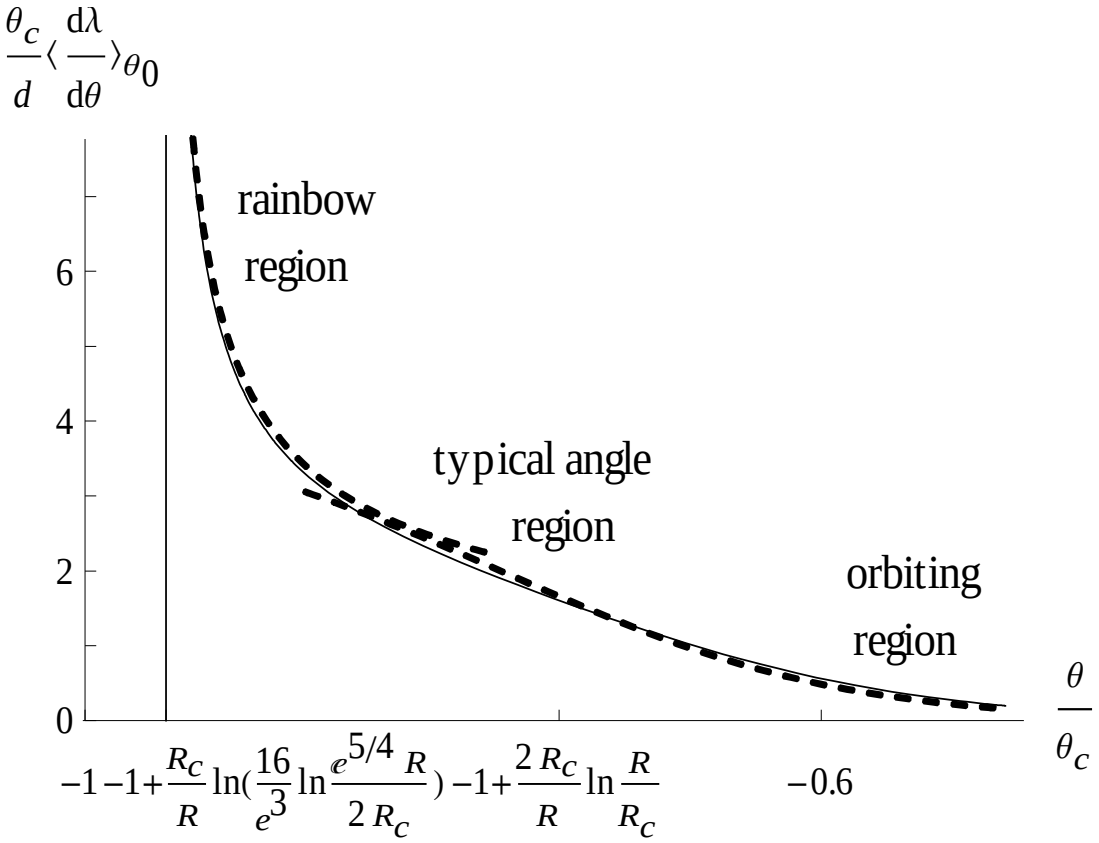

orbiting [Ford & Wheeler, 1959]

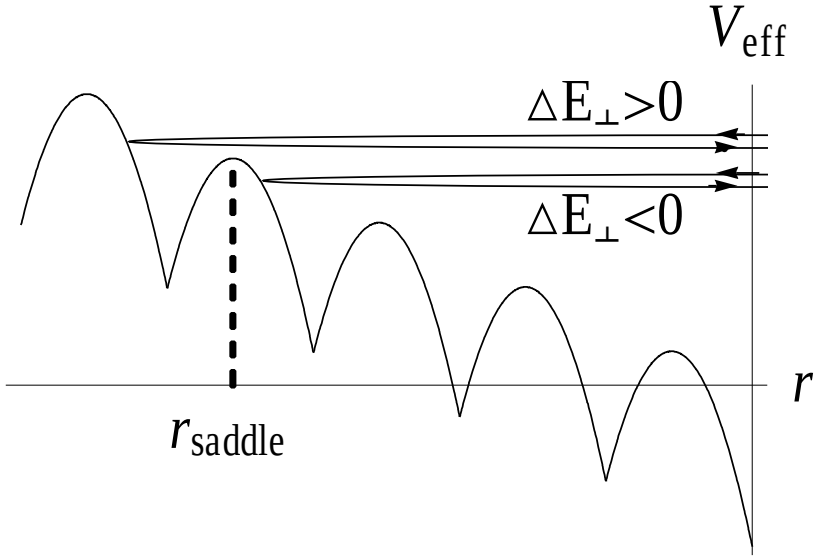

$$\theta \sim \frac{\sqrt{2R_c d}}{R}\begin{cases}\ln\dfrac{V_0}{\Delta E_\perp} & (\Delta E_\perp \to +0)\\ \dfrac{1}{2}\ln\dfrac{R_c V_0}{R|\Delta E_\perp|} & (\Delta E_\perp \to -0)\end{cases}$$

$$\left|\langle\theta\rangle\right| \simeq \left(-1+1.3\frac{R_c}{R}\ln\frac{R_c}{R_c}\right)\theta_c$$

At E=400 GeV, $R/R_c \approx 70$ [CERN, 2009]

$$\begin{cases}\text{Theory}: & \left|\langle\theta\rangle\right| \approx 0.92\theta_c\\ \text{Experiment}: & \left|\langle\theta\rangle\right| \approx 0.66\theta_c\end{cases}$$

Summary for volume reflection. Theory

1. Asymptotic ($R \gg R_c$) values for the volume reflection angle equal: $\frac{\pi}{2}\theta_c$ for positive particles, and θ_c for negative particles. This agrees within 20% with the existing results of numerical simulation using more realistic continuous potentials, and with the CERN experiment for positive particles (though there is an indication of worse agreement for negative particles).
2. The mean volume reflection angle dependence on R_c/R for positive particles is just linear – in general agreement with the CERN experiment.
3. We have proved a statement that boundary effects get completely erased in the differential cross-section averaged over a tiny interval of incident angles, or, analogously, due to a bit of multiple scattering before the volume reflection region. Therewith, the averaging over impact parameters becomes equivalent to averaging over the transverse energy.
4. For negatively charged particles, the final beam profile is asymmetric, exhibiting a spike on its outer edge, corresponding to the rainbow scattering, and an exponential tail on the inner side, corresponding to orbiting. For positive particles, the final beam has a rectangular profile. The intrinsic volume-reflected beam *profile* has not been experimentally accessed yet.

Summary for volume reflection. Experiment

1. For usage of a bent crystal as a coherent beam deflector, one needs a relation between the main parameters

$$\frac{L}{1\text{mm}} < \frac{E}{100\,\text{GeV}} < \frac{R}{\text{m}}, \left(\frac{20\,\mu\text{rad}}{\sigma_0}\right)^2$$

(σ_0 is the r.m.s. angular deviation in the initial beam). The better those inequalities are met, the higher is the deflection quality.

2. If one becomes interested in investigation of the final beam intrinsic *shape*, generated by the continuous potential alone, the above inequalities must be satisfied strongly, but minding the existence of technical lower limits for L and σ_0. This suggests an optimal energy about 50 GeV.

II. Coherent bremsstrahlung in a bent crystal (CBBC)

It will be shown that at over-barrier electron passage through an arbitrarily bent crystal, the accompanying γ-radiation emission in the *bulk* of the crystal (except the vicinities of VR points) is:

1). dipole (i.e., perturbative in the coupling with the external field), as is also typical for coherent bremsstrahlung in straight crystals;

2). for each k is generated around a k-dependent point inside the crystal, within a k-independent length. The latter length is the true coherence length of the process, different from the photon formation length.

In terms of the local crystal curvature $R(z)$, the CBBC radiation spectrum averaged over the electron impact parameters expresses via a single integral over the radiation angle. This integral can be taken explicitly for simple $R(z)$ dependencies – such as a uniform bending, sine-shaped bending, etc.

(As for contribution to radiation from VR point (vicinities), it boils down to suppression of frequencies below the double channeling radiation frequency, causing a dip at the soft end of the spectrum.)

Schematic of an ultra-high-energy particle passage through a thin bent crystal

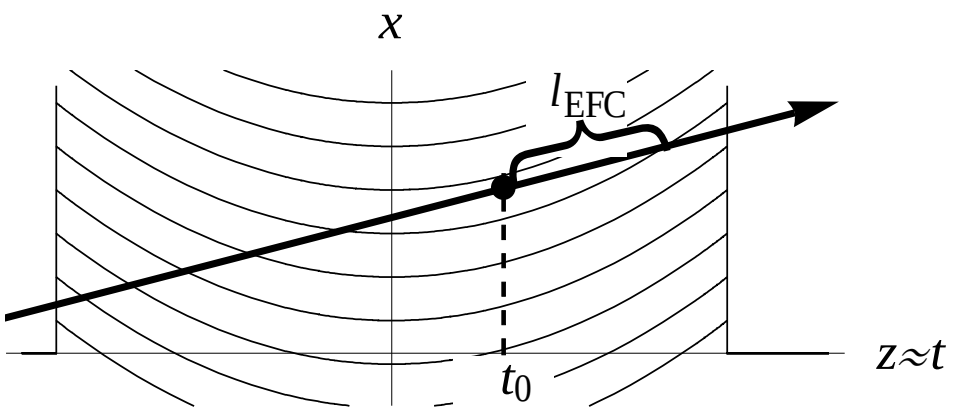

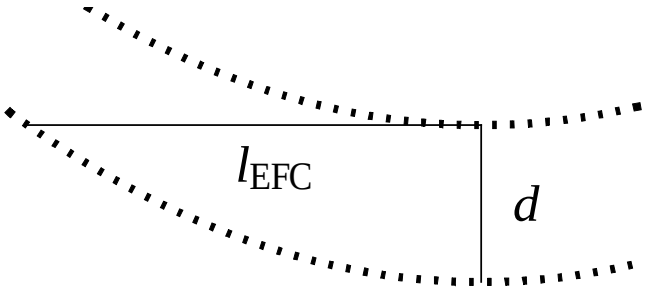

The vicinity of point t_0 of the trajectory tangency to crystal bent planes gives the main contribution to the particle deflection angle.

R – bending radius of active crystallographic planes

d – inter-planar distance

$l_{EFC} = \sqrt{2Rd}$ - coherence length of a fast particle traversing a bent crystal

(different from photon formation length $l_{form} = \dfrac{m^2\omega}{2EE'}$)

Dipole coherent bremsstrahlung in the stationary phase approximation. Analytic formulae

In a crystal bent by an arbitrary profile function $x(z)$, $R(z)=1/\left|x''(z)\right|$.

$$\frac{dE_{CBBC}}{d\omega}=\frac{e^2F_1^2d}{2\pi^3}\frac{E'\omega}{E^3}\sum_{n=1}^{\infty}\frac{c_n^2}{n^{3+2\varepsilon}}\int_{q_{\min}}^{\infty}\frac{dq}{q^2}\left(1+\frac{\omega^2}{2EE'}-\frac{2q_{\min}}{q}+\frac{2q_{\min}^2}{q^2}\right)$$

$$\cdot\left\{\Theta\left(\frac{L}{2}-\left|t_{n+}(q,\theta_0)\right|\right)R\left(t_{n+}(q,\theta_0)\right)+\Theta\left(\frac{L}{2}-\left|t_{n-}(q,\theta_0)\right|\right)R\left(t_{n-}(q,\theta_0)\right)\right\}$$

In a uniformly bent crystal, carrying $R=\text{const}$ out of the integral,

$$\frac{dE_{CBBC}}{d\omega}=\frac{e^2F_1^2Rd}{\pi^3m^2}\frac{E'^2}{E^2}\sum_{n=1}^{\infty}\frac{c_n^2}{n^{3+2\varepsilon}}\left\{\Theta\left(nq_--q_{\min}\right)D\left(\frac{q_{\min}}{nq_-},\frac{\omega}{E}\right)\right.$$

$$\left.+\Theta\left(nq_--q_{\min}\right)\Theta\left(nq_+-q_{\min}\right)D\left(\frac{q_{\min}}{nq_+},\frac{\omega}{E}\right)+\Theta\left(-nq_--q_{\min}\right)\left[D\left(\frac{q_{\min}}{nq_+},\frac{\omega}{E}\right)-D\left(\frac{q_{\min}}{n\left|q_-\right|},\frac{\omega}{E}\right)\right]\right\}\propto l_{EFC}^2$$

with

$$D\left(v,\frac{\omega}{E}\right)=(1-v)\left(\frac{2-v+2v^2}{3}+\frac{\omega^2}{2EE'}\right),\qquad q_{\pm}=\frac{2\pi}{d}\left(\frac{L}{2R}\pm\left|\theta_0\right|\right)$$

Coherent radiation spectra (neglecting multiple scattering and incoherent bremstrahlung), for a definite $\frac{2\pi L\gamma^2}{Rd}$ and several values of $|\theta_0|$.

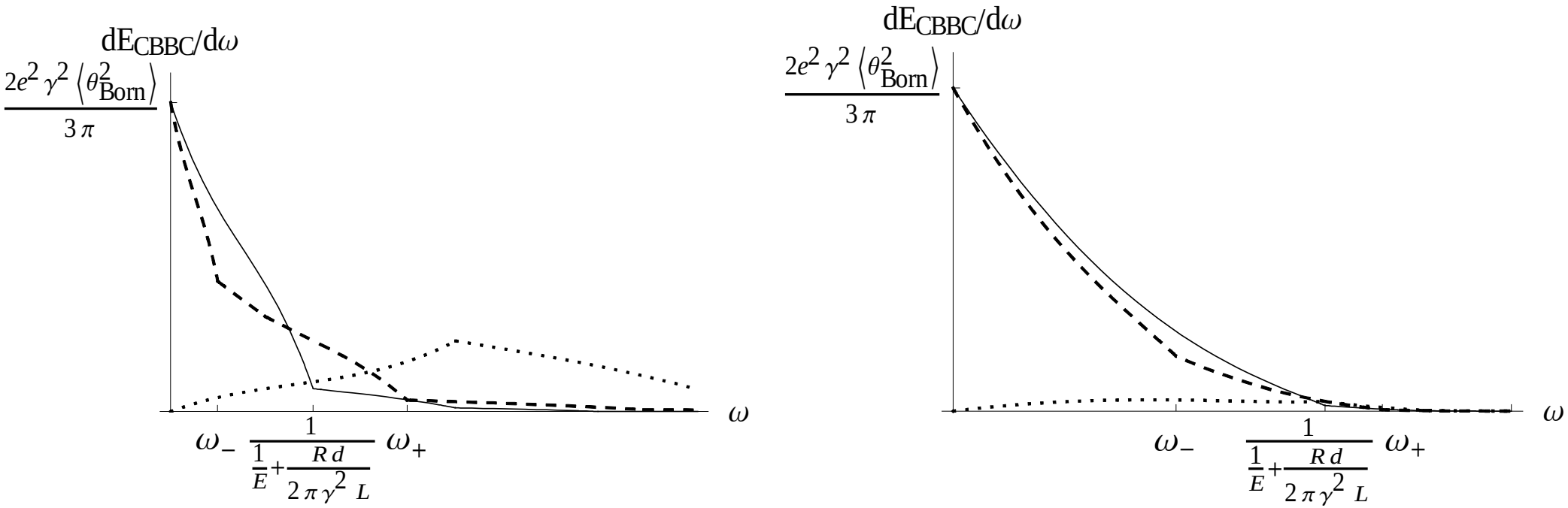

Solid line: $\theta_0 = 0$ (ω_- and ω_+ coincide); dashed: $|\theta_0| = \frac{L}{3R}$; dotted: $|\theta_0| = \frac{L}{R}$.

Left panel: for $\frac{2\pi L\gamma^2}{Rd} \ll E$. Right panel: same as left panel, but for $\frac{2\pi L\gamma^2}{Rd} = 2E$.

The impact of temperature effects on radiation is negligible; the type of crystal orientation ((110) or (111)) mainly affects the frequency and intensity scales.

Volume reflection effect on the radiation spectrum

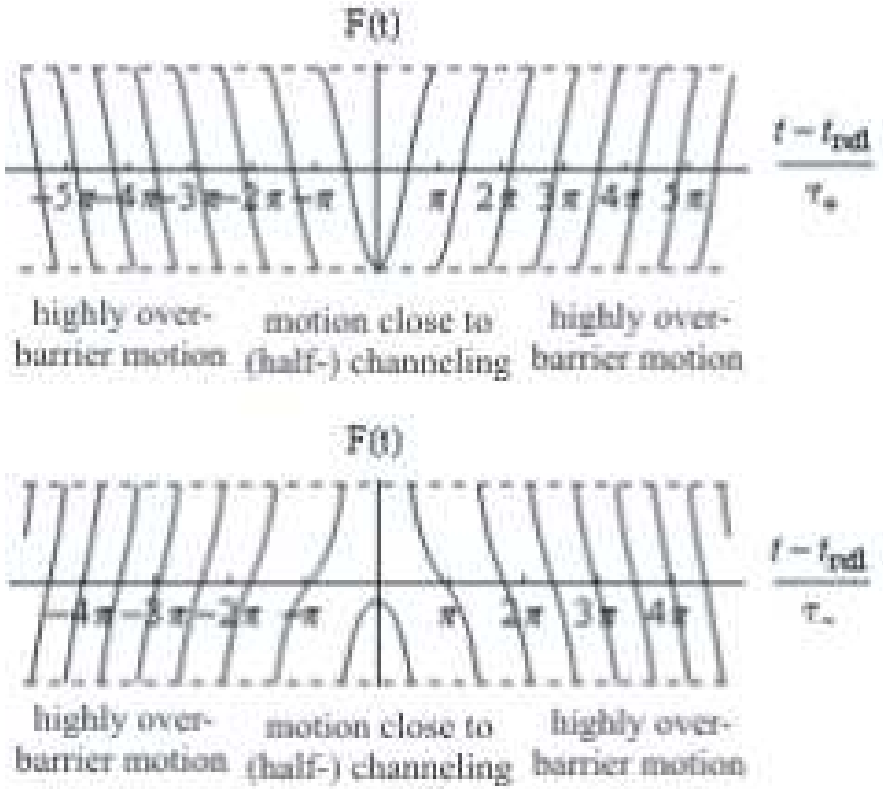

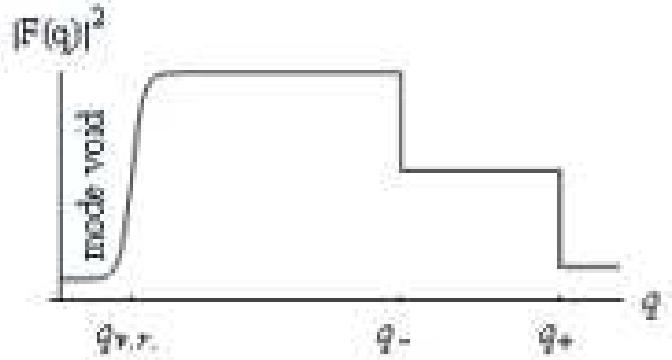

a

b

c

(a) - exemplary graph of time-dependence of the force acting on the crystal on a (positively) charged particle around the volume reflection point, at $R \gg R_c$ (the figure corresponds to $R = 50R_c$). The force discontinuities correspond to the particle passage through (sharp) potential maxima at the atomic plane positions. In vicinity of point $t = t_{refl}$ the trajectory draws nearly tangential to the maximum potential ridge, and in that sense is close to (half-) channeling.

(b) - the same for negatively charged particles. The effective potential maximum is regular ($F \to 0$ on top) and is situated approximately midway the atomic planes.

(c) - schematic of the force Fourier transform modulus square. The dominant contribution to $|F(q)|^2$ and therethrough to $dE_{coh}/d\omega$ comes from the interval $q_{v.r.} \le q \le q_+$.

Schematic of a turnover in the coherent radiation spectrum due to the volume reflection.

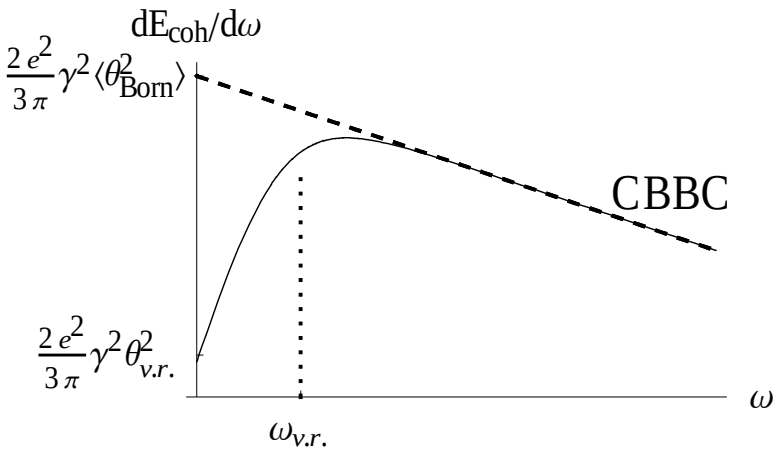

$$\omega_{v.r.} = \frac{1}{\frac{1}{E} + \frac{1}{2\gamma^2 q_{v.r.}}} \qquad q_{v.r.} = \frac{2}{\tau}, \qquad \tau = \begin{cases} \sqrt{\dfrac{2}{R_c d}} & \text{(positively charged particles)} \\ \dfrac{\ln R/R_c}{\pi\sqrt{2R_c d}} & \text{(negatively charged particles)} \end{cases}$$

The modification of the radiation spectrum due to volume reflection is of purely suppressive character and manifests itself as a dip at the soft end of the spectrum. Next to the dip, around frequency $\omega_{v.r.} = \dfrac{1}{\frac{1}{E} + \frac{1}{2\gamma^2 q_{v.r.}}}$ there appears to be a maximum in the spectrum, but it is not to be interpreted as a resonance.

Conditions of applicability

$l_{EFC} = \sqrt{2Rd} \ll L/2$ – the coherence length must be held within the crystal

$\operatorname{var} \Delta x\big|_{|t-t_0|\sim L/2} \ll L/2 \quad \Rightarrow \quad \frac{L}{R} \gg \theta_c$ - the straight passage approximation

$\operatorname{var} \gamma\theta\big|_{|t-t_0|\le L/2} \ll 1 \quad \Rightarrow \quad \frac{L}{R} \gg \theta_V = \frac{V_0}{m} \approx 0.65 \cdot 10^{-4}$ - dipole approximation to rad-n

$\operatorname{var} \theta\big|_{|t-t_0|\sim L/2} \ll \Delta\theta_{mult}\left(l_{EFC}\right) \quad \Rightarrow \quad \frac{L}{R} \ll \theta_V \sqrt{\frac{l_{mult}}{l_{EFC}}}$ - smallness of mult. scat. effect on rad-n

Combining the last two conditions,

$\theta_V \ll \frac{L}{R} \ll \theta_V \sqrt{\frac{l_{mult}}{l_{EFC}}} \quad \Rightarrow \quad$ needs $\sqrt{\frac{l_{mult}}{l_{EFC}}} >>> 1$ (but in practice it is always <10)

Notice: typically $l_{form} = \frac{2EE'}{m^2\omega} \ll l_{EFC}$. Thus LPM condition is less relevant than $l_{EFC} \ll l_{mult}$.

$$\frac{L}{R} \sim \theta_V \left(\frac{l_{mult}}{l_{EFC}}\right)^{1/4} \sim 1.3 \cdot 10^{-4}$$

- There exists an optimal angle for crystal bending

$\gamma\theta\big|_{|t-t_0|\sim L/2} \sim \theta_V \frac{R}{L} \simeq 0.5$ $\qquad$ $\frac{\Delta\theta_{mult}\left(l_{EFC}\right)}{\theta\big|_{|t-t_0|\sim L/2}} \simeq 0.5$

Experimental conditions

Parameters of the bent crystal and incident beam

Experiment	Beam energy, E	Beam divergence	Critical radius, R_c	Critical angle, $\theta_c = \sqrt{d/2R_c}$	Crystal thickness, L	Bending radius, R	Bending angle, L/R
IHEP e^+	10 GeV	0.1 mrad	2.5 cm	80 μrad	0.65 mm	1.3 m	0.5 mrad
CERN e^+	180 GeV	25 μrad	0.5 m	20 μrad	0.84 mm	12 m	70 μrad
CERN e^-	180 GeV	25 μrad	0.5 m	20 μrad	0.90 mm	8 m	110 μrad

Robustness of the dipole CBBC theory

Experiment	Steering quality, R/R_c	Crystal thickness in coherence length units, $L/\sqrt{2Rd}$	Trajectory transverse displacement in lattice constant units, $\frac{4\sqrt{2}R^2 d}{\pi^3 L^2 R_c}$	Non-dipole degree of the radiation, $\frac{R}{L}\tilde{\theta}_V$	Effect of multiple scattering on radiation $\frac{L}{R\tilde{\theta}_V}\sqrt{\frac{\sqrt{2Rd}}{0.13\text{mm}}}$
IHEP e^+	50	23	0.01	0.13	3.5
CERN e^+	27	10	0.03	0.95	0.86
CERN e^-	18	13	0.01	0.6	1.25

Summary for coherent radiation in bent crystals

1. **It is premature to summarize.**
2. **The coherence length in a bent crystal is photon momentum independent.**
3. **To describe the existing experiments analytically, one must learn how to take into account multiple scattering within this length.**